Masonry Arches Simulations Using Cohesion Parameter as Code Enrichment for Limit Analysis Approach

Abstract: A significant number of scientific research groups are still nowadays dealing with masonry material as the main focus of study since it provides an open field of research that is far from resolution in a standardized manner. As masonry structures are highly vulnerable to any level of natural hazards, especially seismic activity, both traditional and composite materials have been used as reinforcements in masonry and provide different solutions that meet the key requirements set out by cultural heritage organizations. Extensive effort has gone into developing appropriate techniques of assessment, that usually demand an individualized methodology of analysis which is to be handled through comparative studies requiring results validation. A suitable field of study is the Limit Analysis approach towards masonry structures, as it offers quite accurate and, more importantly, robust results regarding the necessity to resolve the issues involved in the masonry numerical representation so that reliable outcomes are drawn to enable the assessment of such structures. The enrichment of a Limit Analysis homemade code with the inclusion of cohesion and frictional behaviour at the interface level is able to account, in a simplified but very robust manner, the perplexing issues involved with the numerical assessment of reinforced masonry structures with particular reference to arches. The cohesion incorporation is calibrated for a variety of in-plane applications, accounting for the joints' indirect tensile strength, that is able to simulate the strengthening measures. Results obtained are validated with literature results and included in a comparative study between discrete numerical models that utilize different modelling strategies.

Keywords: Limit Analysis, Friction, No-tension contacts, Cohesion, Reinforced Masonry Arches.

Biographical notes:

1 Introduction

The structural behaviour of masonry is a challenging task considering its composite nature as a material. More particularly when dealing with historical masonry that comprise of dry joints (no mortar) or very weak mortar layers. In such circumstances, the joints act as structural weak points, resulting in a discrete system of blocks. As blocks that form historic masonry are usually with good compressive strength, the assumption that they have infinite compressive strength can be considered. Another reasonable assumption is that the tensile strength of the joints is null, given their extremely low tensile strength. Heyman [1] in his novel Limit Analysis approach considers also the infinite friction and impossibility of sliding along the joints. However, in the case of historic masonry, this assumption for friction is not always realistic, and it is an important element to consider [2, 3]. This is crucial to account, particularly when assessing existing structures.

In recent years a significant amount of interest has been given by diverse authors into tackling this issue. The variety of strategies for the numerical modelling of masonry structures is enormous and each of them contains its specifics with benefits and drawbacks

[4]. The most common and spread techniques consider masonry as a non-linear deformable homogeneous material. Homogeneous modelling does not require special discretization to describe the exact texture, shape and interlocking of the masonry and as such it provides a simplified technique without the need of detailed information on the geometry. However, in order to have a full description and accurately describe the behaviour of masonry, a more detailed constitutive description of such material is required. The drawbacks are that the amount of parameters required in this case is very large and not valid for all types of masonry due to their very diverse nature and as such remains only a rough approximation requiring calibration through experimental testing or other forms of validation. Finite Elements Method (FEM) is among the most common ones dealing with such structures [5, 6, 7, 8]. A more accurate modelling of masonry utilizing such techniques requires the use of fracture mechanics and the ability to account for the development of cracks [9, 10]. However, understanding the anisotropy and the texture dependence of masonry, a recent trend on the simulation of the behaviour of masonry structures is through the help of multi-scale approaches [11, 12, 13, 14, 15, 16] and enriched continuum [17, 18, 19] which are able to account for the micro structure of masonry.

Another popular method is using the macro element models which are more convenient in the assessment of masonry structures for professional use as it is easier to handle larger structures. The main characteristic of the approach consists in the grouping of large panels into piers connected by spandrels and the assessment is done separately for every component disregarding the micro structure. In this scope of models the two main approaches are the equivalent beam-based approach [20, 21] and the spring based approach [22, 23, 24]. In the former masonry panels are represented as nonlinear beams, while in the latter masonry is represented as panels connected with springs.

As stated above, masonry is mainly a discontinuous system of rigid blocks and the most suitable techniques for studying its behaviour are the ones that are able to account for this discrete behaviour in a block-based manner. Such strategies are able to account for the bond behaviour and the actual texture of the masonry regardless of its complexity. Another important feature of such analysis is their ability to localize the weakest spots and the collapsing mechanisms of the entire structure and provide insight for possible interventions. Nevertheless some of these strategies require a huge computational cost and effort to provide results and thus limiting the scale of the studied structure [25, 26], although there are some cases of large scale structures [27, 28]. Nonetheless such efforts are only required while utilizing strategies such as Discrete Elements Method (DEM) [29, 30, 31, 32, 33], FEM with interface elements [34, 35, 36, 37] or Extended Finite Elements Methods (XFEM) [38, 39].

Within the domain of block-based approaches, Limit Analysis (LA) is able to tackle the issue of analysing large structures with discrete textures at a lower computational cost. This approach for masonry has been proposed by Baggio and Trovalusci [2], as a non-standard LA with sliding at the interfaces accounting for friction, in their seminal work and then further proposals have been considered for 2D [40, 41, 42] and 3D [43, 44, 45] structures. Such approaches are able to describe the non-linear behaviour of block masonry with dry joints or filled with weak mortar, taking into account finite frictional resistance. Among a large variety of methods and approaches, LA stands out as a rather simple but powerful method, compared to other approaches in the assessment of existing masonry structures [46, 47]. LA involves a micro model description of masonry units as rigid blocks with joints unable to carry tension and resistant to sliding by friction that account for dry joints or joints with very weak mortar. It has been proven to be especially useful due to the following advantages:

- it enables micro modelling of every block and thus allows considering the geometrical scale influence on the structural response;
- it requires a relatively simple mechanical constitutive model and few input parameters with no need of extensive testing for material characterization;
- it provides straightforward results in terms of collapse multipliers and collapse mechanisms;

An in-house code has been developed at Sapienza University of Rome based on the initial theoretical background of Baggio and Trovalusci [2] named ALMA (*Analisi Limite Murature Attritive*) as a non-standard LA approach considering finite friction for the joint interfaces. The code solves the optimization problem posed by the kinematic upper bound approach as a solution for the minimum collapse multiplier of the assemblage of masonry blocks. Under the consideration of finite friction the optimization problem is subjected to non-linear constraints and obtaining the global minimum is not straightforward. In order to overcome this issue, the problem is linearized by adopting dilatancy and in this way dealing with the associative flow rule. Although this provides an overestimation of the actual global minimum, the solution of the linear problem is very close to the nonlinear one with a large reduction of the computational burden [48].

After an enhancement of the code to include cohesion on the joints, the new capability has been exploited in this paper to simulate the reinforcement of masonry arches by utilizing increased cohesion values as a method for joint reinforcement. Several authors have studied the reinforcement of arches with composite materials. In particular [49, 50, 51] used partial and distributed reinforcements for arch strengthening. In order to validate the ability of ALMA 2.0 to reproduce the strengthening effect of such reinforcements in masonry arches, two examples have been chosen from literature, namely first and second case study. The first case study was originally published by Orduña [52] and then numerically reproduced using different modeling approaches (FEM, DEM and analytical) by Baraldi *et al.* [51] in order to apply and assess the effect of partial reinforcement. The second case study is based on the extensive experimental campaign performed by Oliveira *et al.* [50] whose main objective, among others, was to provide results that may be used as calibration/validation benchmarks for numerical models of composite reinforced masonry arches.

The structure of the paper contains in Section 2 the introduction and the formulations of in-house code ALMA that solves the Limit Analysis problem in the presence of sliding mechanisms. Then, in Section 3 it is presented a case study where a semi-circular arch subjected to a vertical live load is studied using the increased cohesion as reinforcement method and it is compared with benchmarks from literature for the reinforced and unreinforced cases. Another case study is analyzed in Section 4 where a segmental arch subjected to vertical live load is investigated using the same approach and compared to an experimental campaign as a benchmark for both the unreinforced and reinforced cases. Finally, in Section 5 the conclusions and some final remarks are reported.

2 Limit Analysis Code - ALMA 2.0

In ALMA masonry blocks are assumed to be rigid and with a infinite compressive strength, no-tension and frictional joints. Accounting for frictional joints leads towards the non-

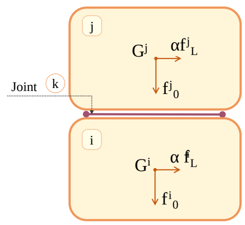

(a) dead and live loads

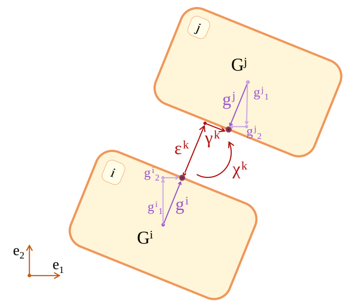

(b) kinematic compatibility

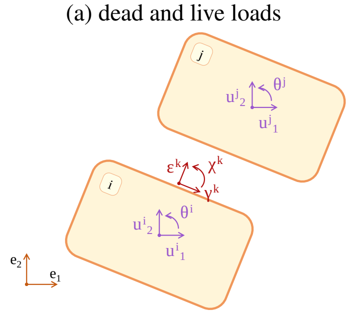

(c) kinematic variables

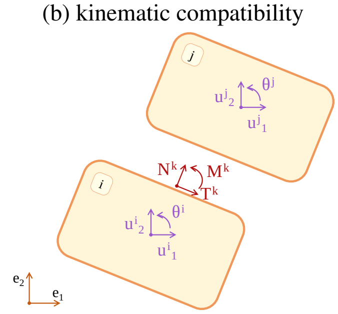

(d) static variables

Figure 1: Limit analysis problem formulation for two blocks

associative case of plasticity as a nonlinear problem in optimization with a duality of solutions. However, the problem is simplified using dilatancy on the joints that results in a linear programming (LP) problem of optimization where associativity and normality rules are assumed.

A recent updating of the code to ALMA 2.0 utilizes more recent programming language as the processor such as *Python* ^{TM} and with the help of various libraries (such as *Mosek*®) [53] is able to solve the upper bound optimization problem formulated. The pre-processing is all carried out in a CAD environment, while the post-processing of the results is achieved in the open source software *Paraview* [54]. The generalized formulation of limit analysis problem for two blocks is shown in Figure 1, namely block i and j with a common interface as joint k, for the case of a horizontal live load. On Figure 1b is shown the kinematic compatibility between the blocks while the kinematic and static variables for joint k are given in Figure 1c and 1d. Considering dilatancy for the joints, the upper bound kinematic approach is solved as a linear programming optimization problem as originally introduced by [2], and after some algebraic operations on the main equations takes optimization problem form as shown in Equations 1.

$$
\begin{aligned}
\alpha_c =& \min \left\{ -\boldsymbol{\lambda}^T \left(\boldsymbol{A}_0 \boldsymbol{N}_1\right)^T \boldsymbol{f}_0 \right\}, & & \\
\textit{subjected to}: & \left(\boldsymbol{A}\boldsymbol{N}_1 - \boldsymbol{N}_2\right)\boldsymbol{\lambda} = \boldsymbol{0}, & \text{(compatibility condition)} & \quad (1)\\
& \boldsymbol{\lambda}^T \left(\boldsymbol{A}_0 \boldsymbol{N}_1\right)^T \boldsymbol{f}_L - 1 = 0, & \text{(positive live load)} & \\
& \boldsymbol{\lambda} \geq \boldsymbol{0} & \text{(bounds on the unknown)} &
\end{aligned}
$$

Utilizing a modified Mohr-Coulomb yield domain it is able to upgrade the code to account different cohesion levels for the joints and indirectly introduce tensile strength on them. This upgrade can be used to account for mortared joints or in the case of very large values of cohesion, it can even account for strengthened joints. This feature is an addition to the various already available code capabilities of ALMA 2.0, namely foundation settlement [47] and retrofitting tie modeling [55]. The new and modified optimization problem takes the form as shown in Equations 2.

$$
\begin{aligned}
\alpha_c = & \min \left\{ \boldsymbol{\lambda}^T [\boldsymbol{c} - (\boldsymbol{A}_0 \boldsymbol{N}_1)^T] \boldsymbol{f}_0 \right\}, & & \\
subjected\ to: & (\boldsymbol{A}\boldsymbol{N}_1 - \boldsymbol{N}_2)\, \boldsymbol{\lambda} = \mathbf{0}, & \text{(compatibility condition)} & \quad (2) \\
& \boldsymbol{\lambda}^T \left(\boldsymbol{A}_0 \boldsymbol{N}_1\right)^T \boldsymbol{f}_L - 1 = 0, & \text{(positive live load)} & \\
& \boldsymbol{\lambda} \geq \mathbf{0} & \text{(bounds on the unknown)} &
\end{aligned}
$$

In the above equations the unknown of the problem remains α_c, a scalar, as the collapse multiplier, with $\boldsymbol{\lambda}$ as the plastic multiplier vector that contains the non-negative coefficients that determine the mode of collapse. $\mathbf{A}_0$ is the inverse matrix of the compatibility kinematic submatrix $\mathbf{B}_1$ of maximum rank while the rest of the kinematic matrix $\mathbf{B}_2$ is stored in the $\mathbf{A}$ matrix as $\mathbf{A} = \mathbf{B}_2\ \mathbf{B}_1^{-1}$. $\mathbf{N}_1$ and $\mathbf{N}_2$ are the submatrices of the block-diagonal gradient matrix $\mathbf{N}$ and correspond to the submatrix of independent and linearly dependent kinematic variables, respectively. $\mathbf{f}_0$ and $\mathbf{f}_L$ are the vectors of the generalized actions on the centres of the blocks for the dead and live loads, respectively. Additional details on the derivations and formulation of the LP problem can be consulted in [48]. Different cohesion values can be assigned to every joint of the masonry assemblage. These values are stored in the form of a vector $\mathbf{c}$. A Mohr-Coulomb classical yield domain is considered with the inclusion of cohesion, thus indirectly involving tensile strength of the joints as $\sigma_t = \mathbf{c}/\tan\phi$, for σ_t as the tensile strength and ϕ as the friction angle. After some algebraic operations the $\mathbf{c}$ vector is stored in the objective function to be minimized through LP.

3 First case study

3.1 Arch and numerical model description

In this first case, a semi-circular arch first studied by Orduña [52] and then by Baraldi *et al.* [51] is considered. The arch has for geometry an internal radius of 235 cm, a ring thickness of 30 cm and an out-of-plane depth of 100 cm. It is composed of 31 voussoirs (see Figure 2). The specific weight of the masonry is 20 kN/m^3, whereas the backfill has a weight of 15 kN/m^3. The friction coefficient between the dry joints is taken as $\tan\phi = 0.75$, as reported on [52]. Finally, null cohesion was considered for all joints.

The loads imposed to the arch consists of its own self-weight, filling material and a concentrated load applied at quarter span factorized with α_c, also called the collapse multiplier, to account for the limit live load of collapse. This live load, in ALMA 2.0, is computed by multiplying the self-weight of one block by α_c. Accordingly, the backfill is modelled utilizing concentrated forces applied to the block joints.

Table 1 Collapse load (in kN) comparison for the first case study arch.

Scenario	**LA Orduña**	**DEM Baraldi *et al.***	**FEM Baraldi *et al.***	**Analytical Baraldi *et al.***	**LA ALMA 2.0**
Unreinforced	18.00	18.00	17.80	17.77	19.67
Reinforced	-	22.00	20.75	23.19	26.84

Orduña modelled the arch using a LA approach and at quarter span, the exact point of live load application, introduced a crack by splitting the block into two pieces allowing for the formation of a hinge at that exact location. On the other hand Baraldi *et al.* [51] studied the same arch, without the split block, using different approaches, namely analytical method, FEM (Finite Elements Method) and DEM (Discrete Elements Method). While Orduña focused only on the unreinforced scenario, Baraldi *et al.* assessed the arch under the unreinforced and reinforced scenarios. In [51] the reinforcement is applied to the joints in between blocks 0 and 14 (see Figure 2), thus partially reinforcing the left haunch of the arch. Similarly, in this work the reinforcement is simulated by applying increased cohesion values to the joints between those blocks.

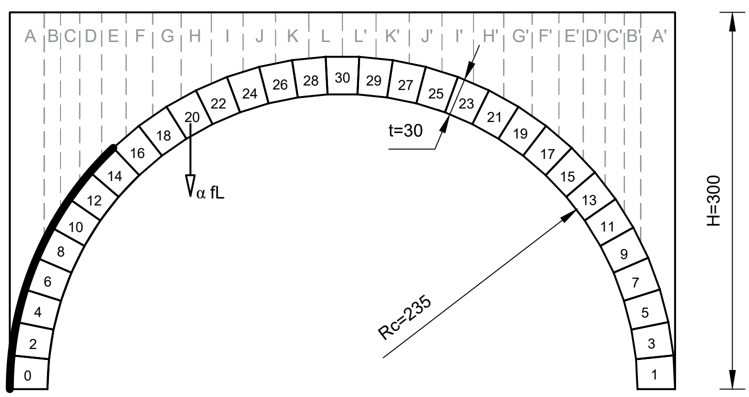

Figure 2: Arch geometry and loading conditions for the first case study reproduced from Orduña [52]

3.2 Results and discussion

Collapse loads are given in Table 1 for both unreinforced and reinforced scenarios as reported by Orduña [52], Baraldi *et al.* [51] and as obtained with ALMA 2.0 in this work. Orduña reported an ultimate load value of 18.0 kN derived by the LA approach, whereas Baraldi *et al.* found comparable values for the FEM approach 18.0 kN and somewhat lower values for the DEM and analytical approaches, 17.8 kN and 17.77 kN, respectively. The collapse load obtained with ALMA 2.0 using was 19.67 kN, that is 9.27 % greater that the reference value achieved by Orduña.

There is a little dissimilarity between the collapse mechanism reported by Orduña and the one derived by ALMA 2.0 for the unreinforced scenario. Hinges H1, H2, and H4 are situated at the same location in both circumstances, as shown in Figure 3. Nevertheless, in the reference example, hinge H3 occurs between blocks 13 and 15 (for reference see Figure 2), but in the ALMA 2.0 result, it appears between blocks 21 and 23. This slight difference of results may be attributed to the division of the block where the concentrated load is applied, as adopted by Orduña. As a result of this modelling choice, in the arch of Orduña hinge H2 occurs at quarter span and the hinge H3 appears at a different place, resulting in a lesser ultimate load. Moreover, there is not information about how the filling material has been modelled in the referenced work and this may cause a significant impact in the results as well.

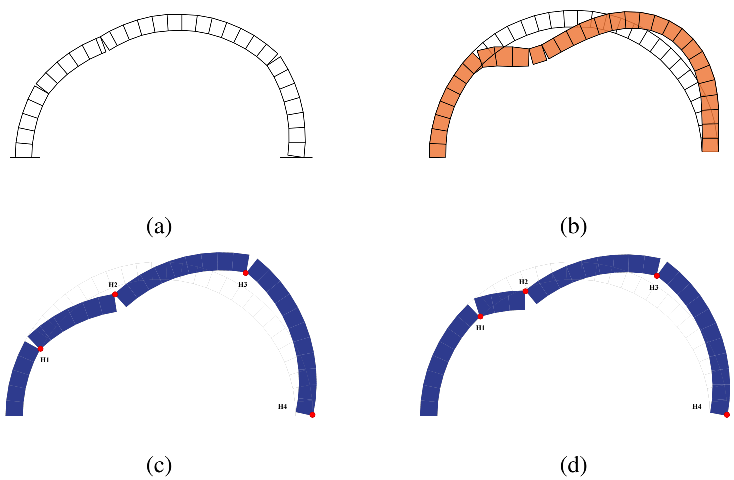

Figure 3: Comparison of collapse mechanisms between Orduña [52]: (a) unreinforced; Baraldi *et al.* [51] (b) reinforced; and ALMA 2.0: (c) unreinforced (d) reinforced.

For the reinforced scenario, the collapse mechanisms obtained by Baraldi *et al.* and the ones determined with ALMA 2.0 are in perfect agreement. It should be emphasized that their modelling decision is the same as in ALMA 2.0, which strengthens the above conclusion for the result on the unreinforced scenario variations. Nonetheless, in this situation, the discrepancy between collapse load values increases, reaching a 29.35 % greater value with ALMA 2.0 than the value obtained for the FEM model of Baraldi *et al*. Finally, as the cohesion value in the joints where reinforcement is applied increases, the location of hinges H1 and H2 shifted, resulting in a larger ultimate load. After reaching a cohesion value of $1.4 \cdot 10^{-4}$ N/mm^2, the collapse load and collapse mechanism are stabilized in the sense that further cohesion increments result in the same collapse load and mechanism. A linear relation between cohesion and collapse load clearly shows this observation for the range of values between 0.00 N/mm^2 to $1.4 \cdot 10^{-4}$ N/mm^2 as can be observed in Figure 4. A normalized collapse multiplier $\hat{\alpha}$ is used for comparable values between the two case studies. This is due to the fact that the collapse multiplier is given in function of the weight of the block to which the load is being applied and the normalization is achieved through the ratio between the self-weight of one block to that of entire arch. Subsequently, a continuous collapse load is achieved regardless of the increment of cohesion value at the reinforced joints.

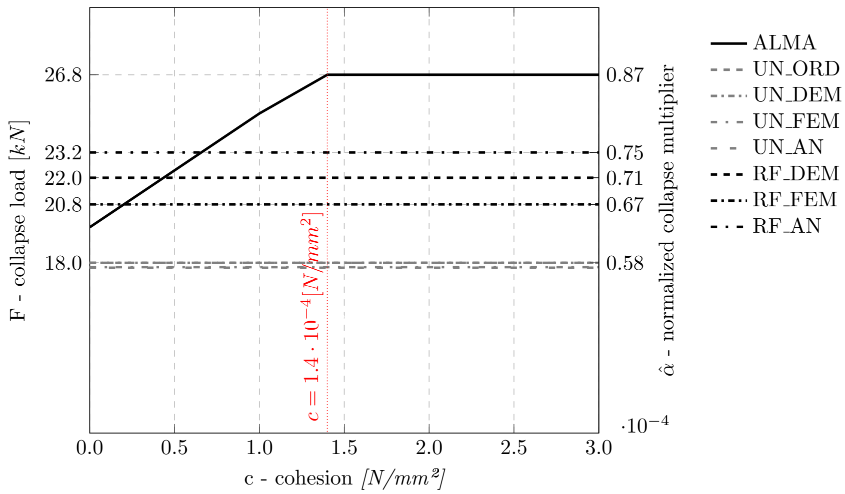

Figure 4: Collapse load (**F**) and normalized collapse multiplier ($\hat{\alpha}$) as a function of the cohesion value (**c**) adopted for the unreinforced (**UN**) and reinfored (**RF**) first case study arches.

4 Second case study

4.1 Arch and numerical model description

The second case study corresponds to the study of an experimentally tested segmental arch [50]. This arch features a 75-cm internal radius, a 45-cm out-of-plane depth and a 5-cm ring thickness. It is made of 59 voussoirs, that form a single ring arch. Two larger blocks at each side of the arch act as supports. The loading conditions comprise the arch self-weight plus a factored concentrated load applied at quarter span (see Figure 5). The value of α, which is used to factor the concentrated load, represents the collapse multiplier required to cause the formation of a collapse mechanism within the context of the LA method implemented within ALMA 2.0.

Two scenarios are considered, namely unreinforced arch and locally reinforced arch. The unreinforced scenario is based on the two arches tested by Oliveira *et al.*, denoted as US1 and US2, whereas the reinforced scenario, LS1 and LS2, encompasses the same two arches but localy reinforced with the use of composites (two 80-mm width GFRP strips placed along the hinges formed in the US arches.). The experimentally reinforced joints, those shown in grey in Figure 5, have been numerically simulated by increasing the inter-block joint's cohesion value. In this way, an indirect tensile strength is applied on these joints accounting for the effect of composite reinforcement.

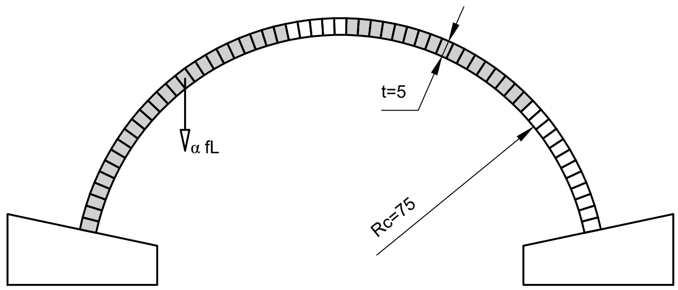

Figure 5: Arch geometry and loading conditions for second case study reproduced from Oliveira *et al.* [50]
.

4.2 Results and discussion

The average values reported by Oliveira *et al.* for both the unreinforced, US_AVG, and the reinforced, LS_AVG, scenarios were used for the calibration purposes of the ALMA 2.0 models provided in this paper.

For the unreinforced scenario, all joints in the LA numerical model were assigned a cohesion value of 0.014 N/mm^2. A satisfactory agreement between the reference findings and the ALMA 2.0 model results was found. The variation was of only 0.6 % (see Table 2). It should be emphasized that no similarity rules were applied for the scaled experimental models during the referenced experimental campaign. This fact might have a significant impact on its outcomes, especially when working with composite materials like masonry. The large value for the cohesion parameter necessary for the model calibration is perhaps also due to the fact that the compressive strengths of the brick and mortar employed in the experimental campaign were almost identical, with bricks having just a 24 % greater compressive strength.

In order to achieve the hinge location shifting observed during the experimental campaign for the reinforced scenario, it was necessary to assign a cohesion value of 0.061 N/mm^2 to the joints reinforced with GFRP (whereas the remainder of the joints were given the same cohesion value of 0.014 N/mm^2 from the unreinforced scenario). After comparing the experimental and numerical collapse loads for the reinforced scenario, the ALMA 2.0 value was 14.53 % greater than the one reported by Oliveira *et al*. This discrepancy might be attributed to the reinforcement characteristics. Whereas the experimental campaign's strengthening consisted of two 8-cm width GFRP strips along the out-of-plane depth of the arch, in ALMA 2.0 the reinforcement includes the entire width of the arch, thus resulting into a slightly tougher structure.

In terms of collapse mechanisms, good agreement was found between experimental and numerical results. For the unreinforced situation, as shown in Figures 6a and 6c, all hinges appear in comparable places, with just a one-block shifting for hinges H4 and H3. With regards to the reinforced scenario, the restriction of hinge opening among the reinforced joints, observed in the experimental specimen, was achieved with the numerical simulation. Moreover, the experimental and ALMA 2.0 collapse mechanisms are alike in terms of the position of hinges H4, H3, and H1. Nonetheless, instead of hinge H2 forming adjacent to

Table 2 Collapse load comparison for the arch reported by Oliveira *et al.* [50].

Scenario	Oliveira et al. [kN]	ALMA 2.0 [kN]	c_1* [N/mm^2]	c_2* [N/mm^2]
Unreinforced	1.68	1.69	0.014	-
Reinforced	2.96	3.39	0.014	0.061

*cohesion value assigned to the unreinforced joints
**cohesion value assigned to the reinforced joints

the right extrados composite reinforcement as seen in the results of Oliveira *et al.*, it opened at the end of the (left) intrados reinforcement for the numerical case.

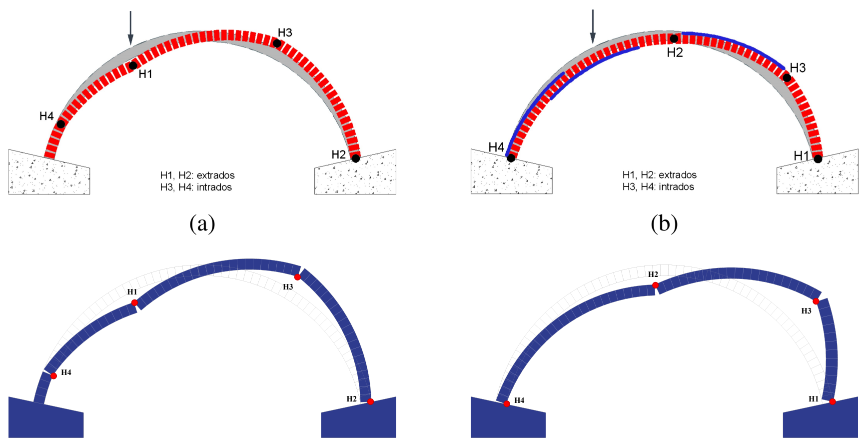

(c) (d)

Figure 6: Collapse mechanisms comparison for the unreinforced case (a) Oliveira *et al.* [50], (c) ALMA 2.0 and reinforced case (b) Oliveira *et al.* [50], (d) ALMA 2.0.

The impact of cohesion value on the collapse load and collapse multiplier is shown in Figure 7. The collapse multiplier in this case is as well normalized $\hat{\alpha}$ with the self-weight of the arch, analogously to the first case study. The unreinforced scenario is represented by the cohesion values ranging from 0 up to 0.014 N/mm^2. The cohesion value only at the reinforced joints is raised after this range until it reaches 0.061 N/mm^2 where the collapse mechanism changes and hinges shift location as previously described. Further increases in the cohesion value of the reinforced joints resulted in the same collapse load and collapse mechanism as all the plastic hinges formed already outside the reinforced joints zone like expected.

5 Final Remarks

Arches with partial composite reinforcement are the focus of this study in validation of the new enrichment of the inhouse code for LA ALMA 2.0. Two examples are considered from literature as benchmarks for the validation and calibration.

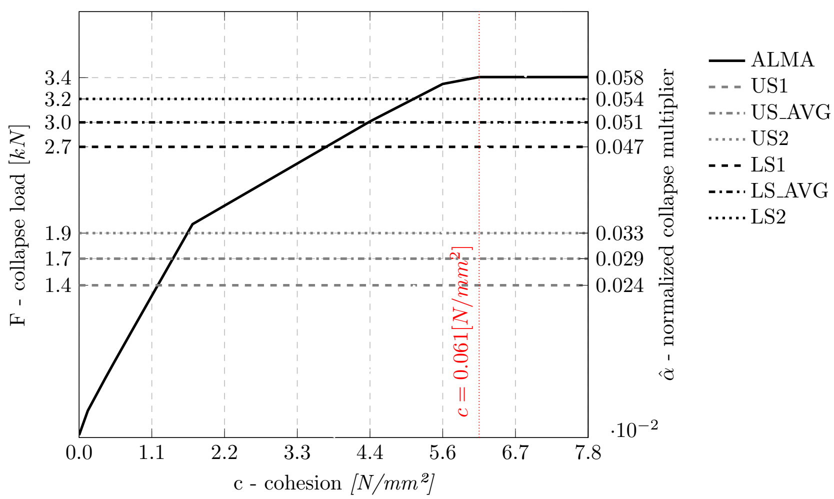

Figure 7: Collapse load (**F**) amd multiplier ($\hat{\alpha}$) as a function of the cohesion (**c**) value adopted for the unreinforced (**US**) and reinforced (**LS**) second case study arches.

A semi-circular arch with a backfill is studied as the first case study that is initially assessed for the unreinforced scenario using LA by [52] and then using FEM, DEM and an analytical approach by [51]. The outcomes of the two studies are in good accordance with ALMA 2.0 where slight discrepancies are observed due to some differences in the original geometry assumptions. Afterwards a partial strengthening technique on the arch extrados of the left support is applied and numerically modelled in FEM, DEM and analytical, where distinctly this measure is able to shift the collapse mechanism into providing higher values for the collapse load. ALMA 2.0 was able to shift the location of the hinge causing the collapse mechanism, and therefore obtaining a higher collapse load value, by increasing the cohesion value of the joints where the reinforcement is applied. Exact collapse mechanisms are achieved with slight differences in the collapse load values with respect to the values reported in the literature.

The second case study corresponds to a segmental arch for which an extensive experimental campaign on scaled models has been conducted and reported by [50]. ALMA 2.0 simulations of the unreinforced and partially reinforced cases reported by Oliveira *et al.* where performed. By utilizing different values of cohesion, it was possible to calibrate the collapse load and obtain similar collapse mechanisms as those of the referenced experimental campaign. Relatively large values of cohesion were necessary to reach the experimental load for both cases. This may have been due to the considerable thickness and resistance of the mortar joints of the experimental models. The average collapse load obtained with ALMA 2.0 for the unreinforced scenario was in perfect correspondence with the value reported in [50]. On the other hand, for the reinforced scenario slightly higher collapse loads were obtained with the LA numerical simulations performed.

It has been shown that improvements and enrichments of LA codes, which require few input parameters, could be capable of providing relatively fast and reliable results for the assessment of composite reinforced masonry arches. Nonetheless, finding strategies and techniques to account for the many impacts that follow the complex nature of masonry structures and their behaviour when strengthened remains an active field of research.

References

[1] J. Heyman. *The Stone Skeleton: Structural Engineering of Masonry Architecture*. Cambridge University Press, 1995.

[2] C. Baggio and P. Trovalusci. Limit analysis for no-tension and frictional three-dimensional discrete systems. *J Struct Mech*, 26, 1998.

[3] A. Jiménez Rios, M. Pingaro, E. Reccia, and P. Trovalusci. Statistical assessment of in-plane masonry panels using limit analysis with sliding mechanism. *Journal of Engineering Mechanics*, 148(2):04021158, 2022.

[4] A. M. D'Altri, V. Sarhosis, G. Milani, J. Rots, S. Cattari, S. Lagomarsino, E. Sacco, A. Tralli, G. Castellazzi, and S. de Miranda. Modeling strategies for the computational analysis of unreinforced masonry structures: Review and classification. *Archives of Computational Methods in Engineering*, 27(4):1153–1185, Sep 2020.

[5] S. S. Ali and A. W. Page. Finite element model for masonry subjected to concentrated loads. *J Struct Eng*, 114, 1988.

[6] M. Bruggi and A. Taliercio. Analysis of no-tension structures under monotonic loading through an energy-based method. *Comput Struct*, 159, 2015.

[7] M. Valente and G. Milani. Seismic assessment of historical masonry towers by means of simplified approaches and standard FEM. *Constr Build Mater*, 108, 2016.

[8] S. Degli Abbati, A. M. D'Altri, D. Ottonelli, G. Castellazzi, S. Cattari, S. Miranda, and S. Lagomarsino. Seismic assessment of interacting structural units in complex historic masonry constructions by nonlinear static analyses. *Comput Struct*, 213, 2019.

[9] J. Toti, V. Gattulli, and E. Sacco. Nonlocal damage propagation in the dynamics of masonry elements. *Comput Struct*, 152, 2015.

[10] S. Saloustros, L. Pelà, and M. Cervera. A crack-tracking technique for localized cohesive-frictional damage. *Eng Fract Mech*, 150, 2015.

[11] S. Pietruszczak and X. Niu. A mathematical description of macroscopic behaviour of brick masonry. *Int J Solids Struct*, 29, 1992.

[12] X. Wei and H. Hao. Numerical derivation of homogenized dynamic masonry material properties with strain rate effects. *Int J Impact Eng*, 36, 2009.

[13] A. Zucchini and P. B. Lourenço. A micro-mechanical homogenisation model for masonry: application to shear walls. *Int J Solids Struct*, 46, 2009.

[14] S. Marfia and E. Sacco. Multiscale damage contact-friction model for periodic masonry walls. *Comput Methods Appl Mech Eng*, 205, 2012.

[15] A. Drougkas, P. Roca, and C. Molins. Analytical micro-modeling of masonry periodic unit cells-elastic properties. *Int J Solids Struct*, 69, 2015.

[16] M. Petracca, L. Pelà, R. Rossi, S. Oller, G. Camata, and E. Spacone. Multiscale computational first order homogenization of thick shells for the analysis of out-of-plane loaded masonry walls. *Comput Methods Appl Mech Eng*, 315, 2017.

[17] R. Masiani and P. Trovalusci. Cosserat and cauchy materials as continuum models of brick masonry. *Meccanica*, 31, 1996.

[18] P. Trovalusci and R. Masiani. Material symmetries of micropolar continua equivalent to lattices. *International Journal of Solids and Structures*, 36(14):2091–2108, 1999.

[19] P. Trovalusci and A. Pau. Derivation of microstructured continua from lattice systems via principle of virtual works: the case of masonry-like materials as micropolar, second gradient and classical continua. *Acta Mechanica*, 225(1):157–177, Jan 2014.

[20] M. Tomaževič. The computer program POR. Technical report, Report ZRMK, Ljubljana (in Slovene), 1978.

[21] Lagomarsino S, Penna A, Galasco A, Cattari S. TREMURI program: Seismic analyses of 3D masonry buildings. Release 2.0, University of Genoa (mailto: tremuri@gmail.com). 2012.

[22] S. Y. Chen, F. Moon, and T. Yi. A macroelement for the nonlinear analysis of in-plane unreinforced masonry piers. *Eng Struct*, 30, 2008.

[23] B. Pantò, F. Cannizzaro, S. Caddemi, and I. Caliò. 3D macro-element modelling approach for seismic assessment of historical masonry churches. *Adv Eng Softw*, 97, 2016.

[24] C. Chácara, F. Cannizzaro, B. Pantò, I. Caliò, and P. B. Lourenço. Assessment of the dynamic response of unreinforced masonry structures using a macroelement modeling approach. *Earthq Eng Struct Dyn*, 2018.

[25] P. B. Lourenço. Computations on historic masonry structures. *Progress in Structural Engineering and Materials*, 4(3):301–319, 2002.

[26] Roca P., Cervera M., Gariup G., and Pela' L. Structural analysis of masonry historical constructions. classical and advanced approaches. *Archives of Computational Methods in Engineering*, 17(3):299 – 325, 2010.

[27] E. Minga, L. Macorini, and B. A. Izzuddin. A 3d mesoscale damage-plasticity approach for masonry structures under cyclic loading. *Meccanica*, 53, 2018.

[28] A. M. D'Altri, F. Messali, J. Rots, G. Castellazzi, and S. Miranda. A damaging block-based model for the analysis of the cyclic behaviour of full-scale masonry structures. *Eng Fract Mech*, 209, 2019.

[29] V. Sarhosis, K. Bagi, J. V. Lemos, and G. Milani. *Computational modeling of masonry structures using the discrete element method*. IGI Global, Pennsylvania, 2016.

[30] E. Çaktı, Ö Saygılı, J. V. Lemos, and C. S. Oliveira. Discrete element modeling of a scaled masonry structure and its validation. *Eng Struct*, 126, 2016.

[31] T. Bui, A. Limam, V. Sarhosis, and M. Hjiaj. Discrete element modelling of the in-plane and out-of-plane behaviour of dry-joint masonry wall constructions. *Eng Struct*, 136, 2017.

[32] J. V. Lemos. Discrete element modeling of masonry structures. *Int J Archit Herit*, 1, 2007.

[33] J. Simon and K. Bagi. Discrete element analysis of the minimum thickness of oval masonry domes. *Int J Archit Herit*, 10, 2016.

[34] P. B. Lourenço and J. G. Rots. Multisurface interface model for analysis of masonry structures. *J Eng Mech*, 123, 1997.

[35] C. Chisari, L. Macorini, C. Amadio, and B. A. Izzuddin. Identification of mesoscale model parameters for brick-masonry. *Int J Solids Struct*, 146, 2018.

[36] D. V. Oliveira and P. B. Lourenço. Implementation and validation of a constitutive model for the cyclic behaviour of interface elements. *Comput Struct*, 82, 2004.

[37] D. Baraldi and A. Cecchi. A full 3d rigid block model for the collapse behaviour of masonry walls. *Eur J Mech-A/Solids*, 64, 2017.

[38] K. F. Abdulla, L. S. Cunningham, and M. Gillie. Simulating masonry wall behaviour using a simplified micro-model approach. *Eng Struct*, 151, 2017.

[39] C. Zhai, X. Wang, J. Kong, S. Li, and L. Xie. Numerical simulation of masonry-infilled rc frames using xfem. *J Struct Eng*, 143, 2017.

[40] M. Ferris and F. Tin-Loi. Limit analysis of frictional block assemblies as a mathematical program with complementarity constraints. *Int J Mech Sci*, 43, 2001.

[41] A. Orduña and P. B. Lourenço. Three-dimensional limit analysis of rigid blocks assemblages. part I: Torsion failure on frictional interfaces and limit analysis formulation. *Int J Solids Struct*, 42, 2005.

[42] A. Orduña and P. B. Lourenço. Three-dimensional limit analysis of rigid blocks assemblages. part II: Load-path following solution procedure and validation. *Int J Solids Struct*, 42, 2005.

[43] A. Orduña. Non-linear static analysis of rigid block models for structural assessment of ancient masonry constructions. *Int J Solids Struct*, 128, 2017.

[44] F. Portioli, C. Casapulla, L. Cascini, M. D'Aniello, and R. Landolfo. Limit analysis by linear programming of 3D masonry structures with associative friction laws and torsion interaction effects. *Arch Appl Mech*, 83, 2013.

[45] F. Portioli, C. Casapulla, M. Gilbert, and L. Cascini. Limit analysis of 3D masonry block structures with non-associative frictional joints using cone programming. *Comput Struct*, 143, 2014.

[46] M. Pepe, M. Pingaro, P. Trovalusci, E. Reccia, and L. Leonetti. Micromodels for the in-plane failure analysis of masonry walls: Limit Analysis, FEM and FEM/DEM approaches. *Frattura ed Integrità Strutturale*, 14(51):504–516, 2019.

[47] M. Pepe, M. Sangirardi, E. Reccia, M. Pingaro, P. Trovalusci, and G. de Felice. Discrete and Continuous Approaches for the Failure Analysis of Masonry Structures Subjected to Settlements. *Frontiers in Built Environment*, 6, 2020.

[48] C. Baggio and P. Trovalusci. Collapse behaviour of three-dimensional brick-block systems using non-linear programming. *Structural Engineering and Mechanics*, 10(2):181–195, 2000.

[49] I. Cancelliere, M. Imbimbo, and E. Sacco. Experimental tests and numerical modeling of reinforced masonry arches. *Engineering Structures*, 32(3):776–792, 2010.

[50] D. V. Oliveira, I. Basilio, and P. B. Lourenço. Experimental behavior of FRP strengthened masonry arches. *Journal of Composites for Construction*, 14(3):312–322, 2010.

[51] D. Baraldi, G. Boscato, C. B. de Carvalho Bello, A. Cecchi, and E. Reccia. Discrete and finite element models for the analysis of unreinforced and partially reinforced masonry arches. In *Mechanics of Masonry Structures Strengthened with Composite Materials III*, volume 817 of *Key Engineering Materials*, pages 229–235. Trans Tech Publications Ltd, 10 2019.

[52] A. Orduña B. *Seismic Assessment of Ancient Masonry Structures by Rigid Blocks Limit Analysis*. PhD thesis, University of Minho, Guimaraes, nov 2003.

[53] MOSEK ApS. *MOSEK Optimizer API for Python 9.3.18*, 2022.

[54] J. Ahrens, B. Geveci, and C. Law. 36 - Paraview: An End-User Tool for Large-Data Visualization. In C. D. Hansen and C. R. Johnson, editors, *Visualization Handbook*, pages 717–731. Butterworth-Heinemann, Burlington, 2005.

[55] M. Pepe. *Numerical modeling for masonry: ALMA 2.0, A computational code for the limit analysis of historical masonry structures*. PhD thesis, Sapienza University of Rome, 2 2020.